A Comprehensive Explanation On The High Quality Characteristics Of Symmetrical Octagonal Spiral Inductor

Ban-Leong Ooi, Dao-Xian Xu, and Pang-Shyan Kooi

MMIC Lab, Dept. of ECE, National University of Singapore, Singapore 119260

Abstract — **Conventional non-symmetrical spiral inductor, which is commonly used in GaAs technology, has limited achievable quality factor when used in silicon LC tanks circuit. As a result, the research of symmetrical, arbitrarily-shaped spiral inductor for silicon technology becomes very important and challenging. However, the detailed mechanism of how the symmetrical, arbitrarily-shaped spiral inductor can achieve a high quality factor is still a mystery. In this paper, we attempt to give a detailed explanation on how the symmetrical, arbitrarily-shaped spiral inductor helps to improve the overall quality factor over that of a traditional, non-symmetrical arbitrarily-shaped spiral inductor. Experimental results are presented to verify our theory. It is hope with this new understanding, alternate forms of symmetrical spiral inductor of high quality factor can be derived.**

I. Introduction

At radio frequency (RF), the usage of on-chip silicon spiral inductors in *LC* tanks circuit is limited by the achievable quality factor (*Q*). The quality factor is seriously affected by three major components. They are the crossover capacitance, the capacitance between the spiral and substrate, and lastly, the substrate capacitance. In the physical modeling of an inductor [2], [3], [5], [7], the series feed-forward capacitance accounts for the capacitance due to the overlap between the spiral and the center-tap underpass [1], [4]. To increase the overall *Q*-factor of the silicon spiral inductor, one usually has to resort to the use of symmetrical spiral inductor, instead of the conventional, non-symmetrical spiral inductor, which is commonly used in GaAs technology. The detailed mechanism of how the symmetrical, arbitrarily-shaped spiral inductor can achieve a high *Q*-factor is still a mystery. In this paper, we attempt to provide a comprehensive explanation on how the symmetrical, arbitrarily-shaped spiral inductor helps to improve the *Q*-factor characteristics over that of the corresponding conventional, non-symmetrical spiral inductor. It is hope with this new understanding, alternate forms of symmetrical spiral inductor can be derived.

II. Theoretical Analysis

A. The Change in C_s

Fig. 1 shows the difference between a symmetrical and non-symmetrical spiral inductor on a silicon substrate. For the ease of explanation, the circuit dimensions corresponding to both types of inductors are assumed to be equal. A typical equivalent circuit model for the non-symmetrical spiral inductor is presented in Fig. 2. In this model, the series branch consists of the spiral inductance, L_s, the metal resistance, R_s and the series feed-forward capacitance, C_s. For most practical inductors, it is sufficient to model C_s as the sum of all overlap capacitances, which is equal to [5]

$$C_s = n \cdot w^2 \cdot \frac{\varepsilon_{ox}}{t_{ox}}, \qquad (1)$$

where n is the number of the overlaps, w is the spiral line-width, ε_{ox} and t_{ox} denote the dielectric constant and thickness of the oxide layer between the spiral inductor and the underpass.

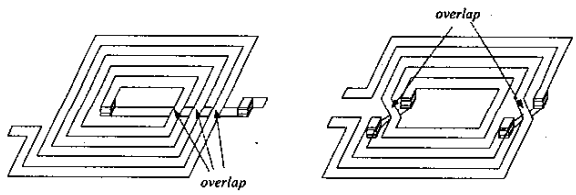

(*a*) (*b*)

Fig. 1. (*a*) A non-symmetrical, spiral inductor. (*b*) A symmetrical, spiral inductor.

Fig. 1 illustrates that for the same inner dimension, width, spacing, and number of turns of a spiral inductor, the symmetrical spiral inductor needs one less overlap than the traditional, non-symmetrical spiral inductor. As such, intuitively, the capacitance, C_s, caused by the overlaps in the symmetrical spiral inductor, will be $1/n$ times smaller than that in the non-symmetrical spiral

0-7803-7694-3/03/$17.00 © 2003 IEEE

inductor. In [1], Yue had expressed the Q-factor of a typical spiral inductor as

$$Q = \frac{\omega L_s}{R_s} \cdot \frac{R_p}{R_p + [(\omega L_s / R_s)^2 + 1] R_s} \cdot \left[1 - R_s^2 (C_s + C_p)/L_s - \omega^2 L_s (C_s + C_p)\right] \quad (2)$$

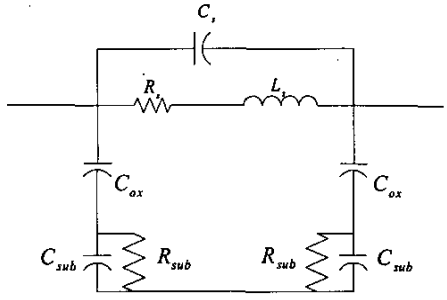

Fig. 2. A typical circuit model for a non-symmetrical spiral inductor.

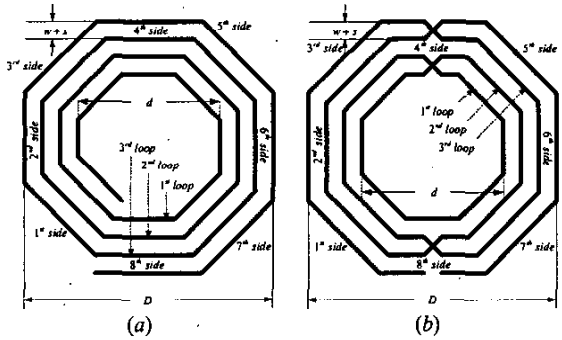

Fig. 3. (a) A non-symmetrical, octagonal spiral inductor. (b) A symmetrical, octagonal spiral inductor.

In this equation, the values of R_p and C_p are irrelevant with respect to C_s. It is obvious that if C_s decreases, the last term $\left[1 - R_s^2 (C_s + C_p)/L_s - \omega^2 L_s (C_s + C_p)\right]$ in equation (2) will increase. This will eventually result in an enhancement on the overall quality factor of the spiral inductor. This conclusion is also valid for an arbitrarily-shaped, symmetrical spiral inductor and as an example, the octagonal symmetrical spiral inductor is referred in the next section.

B. The Change in R_s

The results in [6] showed that the series resistance R_s of the octagonal and circular shaped inductors is smaller by 10% than that of a square-shaped spiral inductor with the same inductance value. In comparison with the square-shaped spiral inductor, from equation (2), one can conclude that the quality factor of both the circular and octagonal spiral inductors will become larger with a decrease in R_s.

As shown in Fig. 3, w, s, and d refer respectively to the width, spacing of the metal trace, and the inner dimension of the spiral inductor. For the same w, s, d, and number of turns n, the difference in the total length of the spiral inductor between the non-symmetrical and symmetrical spiral inductor is about $0.2(n-1)(w+s)$. This factor amounts to less than 1% of the total length of the spiral inductor. As a result of this, with equations (3), (8), and (9) in [8], the self-inductance for both the octagonal, non-symmetrical spiral inductor and the octagonal symmetrical spiral inductor is found to be approximately the same. Thus, the difference in the measured inductance value between the two types of spiral inductor is solely due to the magnetic coupling effect between different arms.

C. The Change in the Magnetic and Electric Center (MEC)

Fig. 4 shows the simplified lumped element model of a typical spiral inductor. In here, we let $l_{i,n}$ and $r_{i,n}$ represent respectively the individual inductance and series resistance observed at the i^{th} side in the n^{th} loop of the spiral inductor. $l_{i,n}$ is the sum of the n^{th} loop self-inductance at the i^{th} side of the spiral inductor and the mutual inductance observed at the i^{th} side. In the case of an octagonal, symmetrical spiral inductor, the *magnetic and electric center* (MEC) is also the geometric center of the inductor. As all the sides of the spiral inductor are equidistant from the MEC, the inter-magnetic coupling observed can be taken to be the same throughout. In this connection, it is naturally to assume that all the $l_{i,n}$s observed on the sides of the spiral inductor will have the same inductance value.

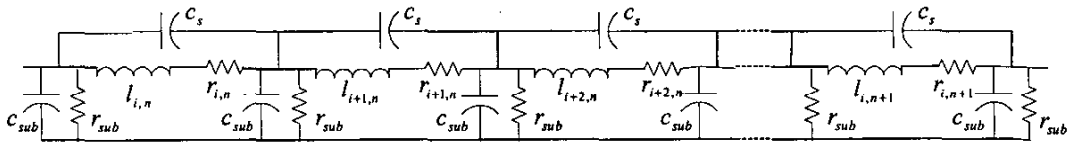

Fig. 4. A simplified lumped element model of a spiral inductor.

Comparing to the non-symmetrical, octagonal spiral inductor, we observe that the non-symmetrical spiral inductor does not have an ideal geometric center. The respective MEC of the spiral inductor is off-set to one side. As such, the magnetic coupling will not be equally distributed throughout the spiral inductor. The half loop that is closer to the MEC will result in larger magnetic coupling and hence, larger values of $l_{i,n}$s in that respective half-loop of the spiral inductor. When the structure is octagonal, one would obtain

$$\begin{cases} l'_{2n-1} = (1-\alpha_n) l_n / 2, \\ l'_{2n} = (1+\alpha_n) l_n / 2, \end{cases} \tag{3}$$

where n=1,2,...,N, l_n refers to the total inductance value of the n^{th} loop in the symmetrical octagonal spiral inductor, N is the maximum number of turn, and α_n is a positive proportionality factor which relates the effect of the off-set MEC to the n^{th} loop symmetrical octagonal spiral inductor. l'_{2n} refers to the mutual inductance value observed by the half n^{th} loop that is closer to the MEC in the non-symmetrical octagonal spiral inductor whereas l'_{2n-1} refers to the mutual inductance value observed by the half n^{th} loop that is further away from the MEC in the non-symmetrical octagonal spiral inductor.

By representing the spiral inductor as a cascade of series networks (See Fig. 4) and neglecting initially the fringing capacitance between opposite side, the whole input impedance of the n^{th} loop of the non-symmetrical spiral inductor in terms of the theoretical *ABCD*-parameters is described as

$$Z'_{in} = A'_{12} = \left[2r_n + \frac{r_n^2 - \omega^2 l_n^2}{r_{sub}} - 2\omega^2 l_n r_n c_{sub} + \frac{\omega^2 l_n^2 \alpha_n^2}{r_{sub}} \right] + j\left[2\omega l_n + \omega c_{sub}(r_n^2 - \omega^2 l_n^2) + \frac{2\omega l_n r_n}{r_{sub}} + \omega^3 c_n l_n^2 \alpha_n^2 \right], \tag{4}$$

whereas for the symmetrical spiral inductor, we obtain

$$Z_{in} = \left[2r_n + (r_n^2 - \omega^2 l_n^2)/r_{sub} - 2\omega^2 l_n r_n c_{sub} \right] + j\left[2\omega l_n + \omega c_{sub}(r_n^2 - \omega^2 l_n^2) + 2\omega l_n r_n / r_{sub} \right] \tag{5}$$

The effective quality factor, Q_{eff}, of a spiral inductor can be calculated from [9] as

$$Q_{eff} = \frac{\mathrm{Im}[Z_{in}]}{\mathrm{Re}[Z_{in}]}, \tag{6}$$

where $\mathrm{Re}[Z_{in}]$ and $\mathrm{Im}[Z_{in}]$ are respectively the real and imaginary parts of the input impedance of a spiral inductor. With equations (4) and (5), we have

$$Q'_{eff} = \frac{\mathrm{Im}[Z'_{in}]}{\mathrm{Re}[Z'_{in}]} < Q_{eff} = \frac{\mathrm{Im}[Z_{in}]}{\mathrm{Re}[Z_{in}]}, \tag{7}$$

when

$$r_n c_{sub} < l_n r_n / (r_{sub})^2 + \omega^2 l_n r_n c_{sub}^2 + l_n / r_{sub}. \tag{8}$$

Q_{eff} and Q'_{eff} denote respectively the *Q-factor* of a symmetrical and non-symmetrical spiral inductor. In practice, c_{sub} is always smaller than $l_n / (r_{sub})^2$. In this connection, the symmetrical, spiral inductor will provide a larger quality factor as compared to the non-symmetrical, spiral inductor.

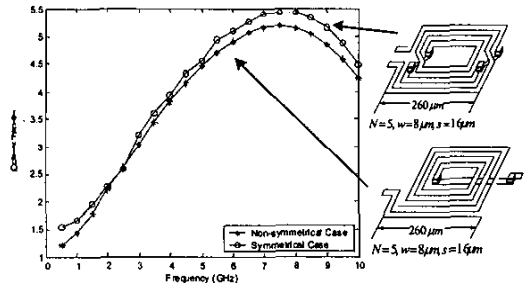

Fig. 5. Comparisons of the quality factors between the symmetrical and the non-symmetrical spiral inductors.

III. Experimental Results

Fig. 5 describes the measured results of the Q of two inductors, symmetrical and non-symmetrical, with 5 turns, 260-μm outer dimension, 8-μm line-width, and 16-μm spacing on the silicon substrate.

We have designed several symmetrical, octagonal spiral inductors having different number of turns or outer dimensions. Except for Inductor_1 to Inductor_3, which have 3 turns each, all the other inductors have 5 turns. The outer dimensions of these inductors, numbered from Inductor_1 to Inductor_7, are 200-μm, 250-μm, 300-μm, 150-μm, 200-μm, 250-μm, and 300-μm, respectively. All these inductors have 8-μm line-width and 4-μm spacing between the turns, and they were fabricated on two layers of semi-conductors. The thickness of the upper SiO_2 layer is 20-μm, and the thickness of the lower silicon layer is 50-μm. The *S*-parameters are measured up to 10 GHz with IC-CAP.

Fig. 6 shows the measured quality factors of our inductors. Within the group of inductors with the same number of turns, the maximum quality factor observed belongs to the smallest spiral inductor, which has a shorter length of metal trace. With C_s remained

relatively unchanged within the group, this high quality factor is mainly due to the lower R_s value observed for smaller spiral inductor.

At low frequency (particularly lower than 2 GHz), the *Q-factor* can be well described by $\omega L_s / R_s$ as the last two terms in equation (2) have values close to unity [1]. From Fig. 6, it is noted that with an increase in the length of the spiral inductor within the group of same number of turns, the inductance values increase faster than the series resistance. Moreover, with a larger outer dimension, the inductance value, L_s, is higher. With an increase in frequency, the eddy currents [10] will become larger and hence, the resistance, R_s, will also increase. With this, the overall Q-factor becomes progressively smaller at relatively high frequencies.

From Fig. 6, we also noted that in case of the same number of turns, the measured resonant frequencies decrease with an increase in the outer dimensions (from Inductor_1 to Inductor_3, and from Inductor_4 to Inductor_7). With an increase in the outer dimensions, more overlaps are resulted and thus, the effect due to the capacitance C_s becomes pre-dominant. The theoretical resonant frequency, derived from the last term of expression (2) is

$$f_{res} = \frac{1}{2\pi}\sqrt{\frac{L_s - R_s^2(C_s + C_p)}{L_s^2(C_s + C_p)}}. \quad (9)$$

This expression shows that with an increase in C_s, the overall resonance frequency will decrease. Within the group of same outer dimensions, the capacitance, C_s, will become larger when the number of turns increases. As a result, this usually constitutes a decrease in both the maximum quality factor and the f_{res} (See Fig. 6).

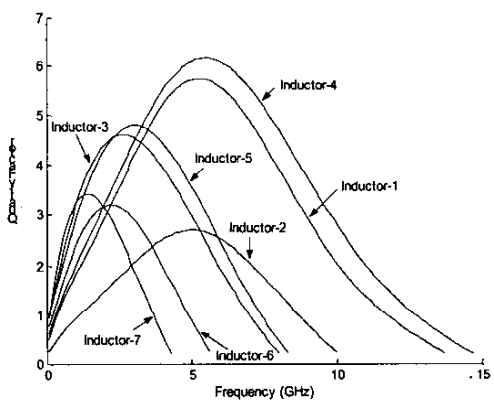

Fig. 6. Quality factors for various spiral inductors.

IV. Conclusion

Compared with the non-symmetrical structure, symmetrical octagonal spiral inductors can reduce the coupling capacitance from the overlaps of the spirals. Furthermore, the EMC of the symmetric case may be the accurate geometric center of the spiral inductors that may balance the effect of inductance coupling between different parts of the spiral. All these aspects will provide high quality factors and resonance frequencies of the inductors. The number of overlaps will reduce the Q in high frequency domain. However, in low frequency domain, the prominent factor which influences Q is the outer dimension which affects more on the increasing of inductance than the resistance in case of the same number of turns.

References

[1] C. P. Yue and S. S. Wong, "On-chip spiral inductors with patterned ground shields for Si-based RF IC's," *IEEE J. Solid-State Circuits*, vol. 33, pp. 743-752, May 1998.

[2] J. R. Long and M. A. Copeland, "The modeling, characterization, and design of monolithic inductors for silicon RF IC's," *IEEE J. Solid-State Circuits*, vol. 32, pp. 357-369, Mar. 1997.

[3] H. M. Greenhouse, "Design of planar rectangular microelectronic inductors," *IEEE Trans. Parts, Hybrids, Packaging*, vol. PHP-10, pp. 101-109, June 1974.

[4] L. Wiemer and R. H. Jansen, "Determination of coupling capacitance of underpass, air bridges and crossings in MIC's and MMIC's," *Electron. Lett.*, bol. 23, pp. 344-346, Mar. 1987.

[5] C. P. Yue and S. S. Wong, "Physical modeling of spiral inductors on silicon," *IEEE Transactions on Electron Devices*, vol. 47, pp. 560-568, No. 3, Mar. 2000.

[6] S. Chaki, S. Aono, N. Andoh, Y. Sasaki, N. Tanino, and O. Ishihara, "Experimental study on spiral inductors," in *IEEE MTT-S Int. Microwave Symp. Dig.*, pp. 753-756, June 1995.

[7] F. W. Grover, *Inductance Calculation*, New Yor,k, NY: Van Nostrand, 1962.

[8] S. Jenei, B. K. J. C. Nauwelaers, and S. Decoutere, "Physics-based closed-form inductance expressions for compact modeling of integrated spiral inductors," *IEEE J. Solid-State Circuits*, vol. 37, pp. 77-80, Jan. 2002.

[9] J. N. Burghartz, "Spiral inductors on silicon-status and trends," *Int. J. RF Microwave Computer-Aided Eng.*, vol. 8, pp. 422-432, Nov. 1998.

[10] W. B. Kuhn and N. M. Ibrahim, "Analysis of current crowding effects in multiturn spiral inductors," *IEEE Transactions on Microwave Theory and Techniques*, vol. 49, No. 1, pp. 31-38, Jan. 2001.